

Research Article

Curing Dynamics of Soy Flour-Based Adhesives Enhanced by Waterborne Polyurethane

Yong Wang ^{1,2}, Xianjun Li ², Wanli Lou ³, Layun Deng ¹ and Youhua Fan ¹

¹Key Laboratory of State Forestry Administration on Utilization Science for Southern Woody Oil Resource, Hunan Academy of Forestry, Changsha, Hunan Province, China

²College of Materials Science and Engineering, Central South University of Forestry and Technology, Changsha, Hunan Province, China

³Torch High Technology Industry Development Center, Ministry of Science & Technology, Beijing, China

Correspondence should be addressed to Youhua Fan; yh_fan@163.com

Received 12 July 2018; Accepted 16 December 2018; Published 31 January 2019

Academic Editor: Domenico Acierno

Copyright © 2019 Yong Wang et al. This is an open access article distributed under the Creative Commons Attribution License, which permits unrestricted use, distribution, and reproduction in any medium, provided the original work is properly cited.

In this paper, thermogravimetric (TG) analysis was carried out to make clear the curing properties of soy flour-based adhesives (SFAs) enhanced by waterborne polyurethane (WPU) with different addition levels. The kinetic parameters were evaluated by a thermal dynamics method, including activation energy and preexponential factor. In addition, the structure characteristics of both soy flour and modified soy flour-based adhesives were tested by Fourier transform infrared spectroscopy (FTIR). The results revealed that the FTIR spectra of pristine soy flour-based adhesives were different from those of soy flour after alkali treatment and waterborne polyurethane modification. Furthermore, there were four main degradation phases in the derivative thermogravimetric (DTG) curves of modified soy-based adhesives while there were two phases of a defatted soy flour sample. The kinetics analysis demonstrated that the curing process could be described as a consecutive first-order curing process. Moreover, with the addition level of WPU growing, the apparent activation energy of each phase of the curing process was increasing compared with that in pristine soy-based adhesives.

1. Introduction

Much work on wood adhesives in recent years has been focused on the substitution of traditional petrochemical-based resins such as urea formaldehyde resin, phenol formaldehyde resin, and melamine formaldehyde resin, which can induce potential detriment of formaldehyde released from plywood panels. In response to the concern on a new type of formaldehyde-free adhesives, great attentions have been paid to wood adhesives prepared from renewable and natural materials without formaldehyde addition, including starch and soy flour [1–3]. Most studies have been based on these two materials, which are both abundant and effective in the preparation of formaldehyde-free adhesives [4, 5]. However, starch is mainly derived from foodstuff such as rice, wheat, and potato, threatening the normal food supply of humans. Therefore, soy flour that is not edible directly as the by-product of soy oil production is abundant, affordable,

and readily available for the preparation of wood adhesive [6]. Although soy flour is prospective to be applied for preparation of wood adhesive, the scope of its applications is restricted for its poor water resistance compared with traditional wood adhesives. Consequently, it is important and necessary to employ various methods to prepare high water-resistance SFAs. Soy flour is composed of polysaccharides and soy protein; thereinto, soy protein mainly consisted of twenty different kinds of amino acids, which contain functional and active groups bonded in branched chains of polypeptide, comprising carboxyl (-COOH), hydroxyl (-OH), amino (-NH₂), etc. [7]. Various chemical reactions are possible due to these functional and active groups. Therefore, it is widely accepted to employ chemical methods to prepare high-performance SFAs in order to broaden the scope of its applications.

At first, researchers used alkali [8], urea [9], sodium dodecyl sulfate (SDS) [4], and sodium dodecyl benzene

sulfonate (SDBS) [10] to break down the structure of soy protein to enhance bonding strength and water resistance of SFAs. However, the wet shear strength of wood panels adhered by these adhesives did not meet the requirements of type II application (≥ 0.7 MPa). As an alternative, grafting modification was employed to enhance the water resistance of SFAs. Much work mainly applied maleic anhydride (MA) to graft soy protein in order to enhance its reactivity during hot pressing [11]. Although the grafting method was effective to prepare high-performance SFAs, it was time-consuming and expensive for large-scale industrial production. On the other hand, cross-linking modification has attracted growing attentions in recent years. A large number of cross-linking agents with high efficiency were developed to improve the water resistance of SFAs, such as itonic acid-based PAE [12], 2-octen-1-ylsuccinic anhydride [13], undecylenic acid [14], isocyanate, and other resins [15, 16], all of which were proven to be effective approaches to develop high-water-resistance adhesives. However, little attention has been paid to the curing kinetics of SFAs. In our previous research, waterborne polyurethane (WPU) was employed as a cross-linking agent and certified to be effective to improve water resistance significantly [17]. For further study on curing kinetics, WPU was also used as a cross-linking agent to modify soy-based adhesives. In order to clearly understand the reaction mechanism, the thermal degradation kinetics of the adhesive was attempted to study. Through the analysis of the experimental data by the Coats-Redfern integral method, the mechanism of the curing process and the kinetic model were determined, and the kinetic parameters were also obtained.

2. Materials and Methods

2.1. Materials. The main material was soy flour and provided by Xianglin Food Co. Ltd., China, with 12% moisture and around 52% protein content. WPU purchased from Guanzhi New Material Technology Co. has a solid content of 38%, a pH of 7-9, and a viscosity of 100-200 mPa·s. All other chemical reagents were chemically pure and purchased from Sinopharm Chemical Reagent Co. Ltd., China. Poplar veneers with the dimensions of 600 mm \times 600 mm \times 1.8 mm (width \times length \times thickness) were supplied by Fusen Wood Industry Co. Ltd., China. The moisture content of wood veneers was 8-12%.

2.2. Preparation of SFAs. One 500 ml flask with three necks installed with a mechanic stirrer, a condenser, and a thermometer was added with distilled water (190.5 g), sodium hydroxide (7.5 g), and urea (3.0 g). All chemicals and materials were blended together, and then soy flour (99 g) was slowly added to the flask with rapid stirring until complete dissolution. Different amounts (5%, 10%, 15%, and 20%) of WPU were added into the SFA slurry.

2.3. Fourier Transform Infrared Spectroscopy. FTIR spectra of soy flour and SFAs were recorded with the NICOLET-is5 spectrometer (Thermo Fisher, USA). All adhesive samples were first cured in the oven at 140°C for 2 h and ground into

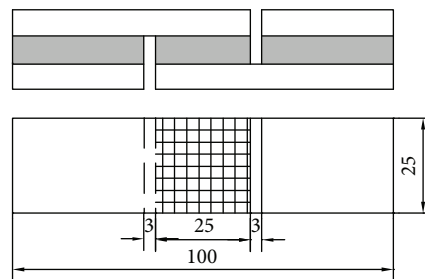


FIGURE 1: Sample size of the shear strength test.

powder over 200-mesh sieves. 16 scans were performed with a 4 cm^{-1} resolution over the range of 650 to 4000 cm^{-1} , using an attenuated total reflectance (ATR) accessory.

2.4. Thermogravimetric Analysis. The adhesive samples were first vacuum freeze-dried for 72 h and ground into powder over 120-mesh sieves. Thermal analysis of the adhesive samples was implemented by using a Netzsch STA-449C thermogravimetric analyzer at a heating speed of $10^\circ\text{C}/\text{min}$ in the range of 30-800°C under nitrogen flow with a constant speed of 40 ml/min.

2.5. Preparation of Plywood Samples. Three-layer plywood samples ($300 \times 300 \text{ cm}^2$) were fabricated with $320 \text{ g}/\text{m}^2$ of SFAs (wet weight basis) coated on each layer of the poplar veneer. This adhesive-coated veneer was stacked between two uncoated ones with the grain directions of two adjacent veneers perpendicular to each other. Afterwards, these assembled three-layer plywood samples were cold-pressed at 1.0 MPa for 30 min under room temperature and next hot-pressed at 1.2 MPa and 85 s/mm at 130°C . After hot pressing, the panels were stored at ambient temperature for 24 h before evaluation.

2.6. Shear Strength Test. Figure 1 provides the shape of the test sample, which was prepared in accordance with Chinese National Standard GB/T 9846.7-2004, and the shear strength test complied with Chinese National Standard GB/T 17657-1999. The dry shear strength of the samples was investigated by a universal strength testing machine (Jinan Shijin Co. Ltd., China) with a cross-head rate of 2.0 mm/min. The following method was how to measure the wet shear strength of the samples: six parallel samples were soaked in water at 63°C for 3 h, and next these samples were measured using the same method of dry shear strength after cooling at room temperature for 10 min. All data was compared by average value.

3. Results and Discussion

3.1. Analysis of Shear Strength. The shear strength of samples bonded by SFAs is provided in Table 1. It could be concluded that the wet shear strength was improving with the WPU addition level increasing after treatment, and when the addition level of WPU was over 10 wt.%, the samples met the requirements of type II plywood application. It revealed that adding WPU had a direct relationship with the properties of

TABLE 1: Shear strength of SFAs.

	SFA	SFA+WPU5	SFA+WPU10	SFA+WPU15	SFA+WPU20
Dry shear strength (MPa)	0.85	0.87	0.90	1.04	1.12
Wet shear strength (MPa)	—	0.65	0.71	0.84	0.90

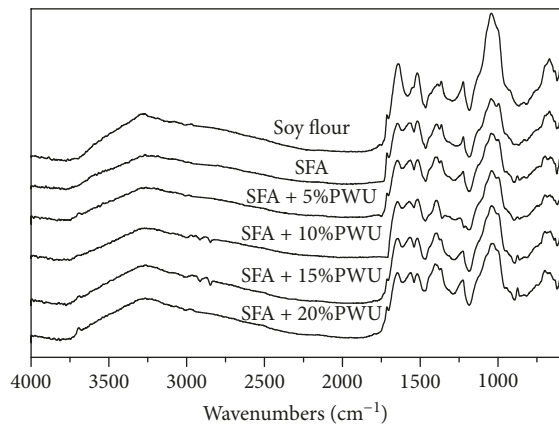


FIGURE 2: FTIR spectra of soy flour and SFAs.

SFAs. Furthermore, the molecule of SFAs could react with WPU and formed the network structure that water could not penetrate the bonding layer. Therefore, the water resistance and bonding strength of SFAs with WPU modification could be enhanced significantly.

3.2. FTIR Analysis. FTIR spectra of soy flour and SFAs are illustrated in Figure 2. During the curing process, WPU as the cross-linking agent contained both the amide group and hydroxide group and could react with proteins, polysaccharide, and wood substrate [18]. Moreover, after curing reactions, the network structure was formed in the bonding layer with the decline in hydrophilic groups that could enhance water resistance of SFAs significantly. The characteristic absorption peaks of soy protein including amide I, amide II, amide III occurred at 1648, 1520, 1221 cm^{-1} , corresponding to C=O stretching, C-N stretching, and N-H bending vibration, respectively [19, 20]. Furthermore, the characteristic absorption bands of the carboxyl group (COO-) and amide group (-C-NH₂) were observed at 1363 cm^{-1} and 1036 cm^{-1} . However, the key distinction between the FTIR spectra of soy flour and all SFA samples occurred at 1560 cm^{-1} and 1363 cm^{-1} . The absorption band of amide II (1518 cm^{-1}) was divided into two peaks, and one of them was red-shifted to lower wavenumbers (1560 cm^{-1}) along with the addition level of WPU rising, indicating new intermolecular interactions generated between the soy protein and WPU molecule. Moreover, the absorption band of COO- stretching vibration occurred at 1363 cm^{-1} and was also red-shifted to lower wavenumbers (1391 cm^{-1}) along with the addition level of WPU growing, which also revealed new intermolecular bonds between the soy protein and WPU molecule. The probable scheme of cross-linking reaction between soy flour and WPU is illustrated in Figure 3. WPU performed as the cross-linker in soy-based adhesives. During

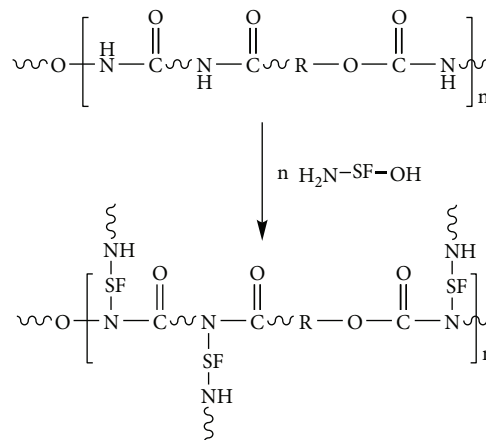


FIGURE 3: Ideal scheme of curing reaction between soy flour and WPU.

the curing process, the macromolecule of WPU could react with soy protein. Thus, soy protein could be connected together by WPU to form an interpenetrating network structure, which could enhance the water resistance of modified SFAs.

3.3. Characterization of Curing Property. The TG and DTG curves of SFAs are illustrated in Figure 4. Compared with the DTG curve of pristine SFAs, the DTG curves of SFAs with WPU modification experienced a four-phase process, which were different from those of SFAs with only two-phase process. For SFAs, the first phase from 30.0 to 148.2°C was mainly assigned to the volatilization of bonded water and small organic matter including alcohols [21]. At the second phase from 258 to 381°C, the protein chains and polysaccharide of SFAs were degraded completely, accompanied by emission of various gases such as CO, NH₃, and CO₂ [22]. Different from pristine SFAs, modified SFAs experienced the similar bonded water loss and protein decomposition phase, and the cross-linking reaction was taking place in the first phase for modified SFAs. However, with WPU modification, two more phases were observed at 186-220°C and 394-453°C separately. The second phase of SFAs with WPU modification occurring at 186-220°C was mainly ascribed to the degradation and volatilization of the small molecule part of WPU. The fourth phase emerging at ~400°C was due to the polyol decomposition [23]. Moreover, after modification with WPU, the peak in the third phase was split into two peaks, and the degradation process of modified SFAs was also mainly taking place in this phase.

The main compositions of defatted soy flour are soy protein and polysaccharide. For pristine SFAs, in the degradation process, soy protein and polysaccharide were pyrolyzed with temperature growing, accompanied by emission of

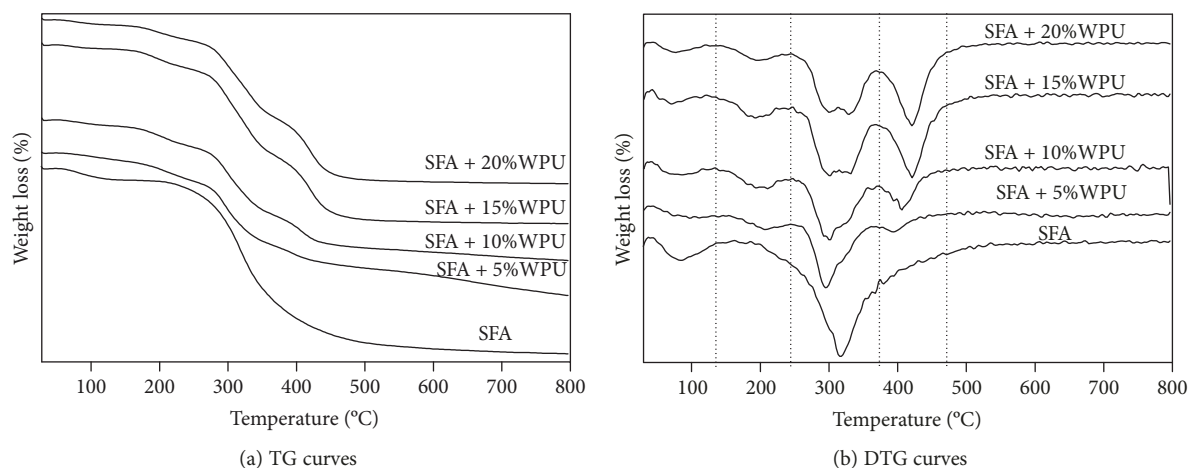


FIGURE 4: TG and DTG curves of different adhesive samples.

TABLE 2: Characteristic temperatures and maximum weight loss speeds of SFAs.

Samples	Characteristic temperatures				$(dW_1/dt)_{\max}$	$(dW_i/dt)_{\max}$ ($\% \cdot \text{min}^{-1}$)			Residue ratio (%) TG (800°C)
	T_1 (°C)	T_2 (°C)	T_3 (°C)	T_4 (°C)		$(dW_2/dt)_{\max}$	$(dW_3/dt)_{\max}$	$(dW_4/dt)_{\max}$	
SFA	87.9	/	316.7	/	-1.44	/	-8.33	/	1.2
SFA-WPU5	86.8	210.2	298.3	393.3	-0.62	-1.57	-5.54	-1.75	2.3
SFA-WPU10	84.8	207.8	301.1	405.4	-0.71	-1.72	-5.36	-3.22	3.5
SFA-WPU15	78.6	196.1	301.2/332.1	421	-0.68	-1.74	-5.82/-5.71	-5.99	4.4
SFA-WPU20	76.2	195.7	299.7/328.6	420	-0.69	-1.27	-5/-5.15	-5.96	4.2

Note: $(dW_i/dt)_{\max}$ is the value of the maximum weight loss ratio.

various gases [24]. For modified SFAs, the polyols of WPU were decomposed to various small molecule compounds including CO_2 , CO, alcohols, and aldehydes, and the cleavage of ester bonds and amino methyl ester bonds also took place simultaneously when the temperature was over 380°C in the degradation process [25, 26]. When the temperature was low ($<240^\circ\text{C}$), WPU could react with soy protein and come into being polymers which made the degradation temperature higher and acquire better thermal stability. It could be seen from Figure 4(b) that compared with SFAs, there were two peaks of maximum weight loss rate for the modified SFAs in the third phase. The first peak decreased with WPU addition level rising while the second peak was shifted to the high-temperature area. These results verified that there was the formation of the polymers between the soy protein and WPU molecule after cross-linking reaction and these polymers mainly decomposed beyond 320°C in the degradation process, indicating better thermal stability of modified SFAs [27].

The maximum weight loss speed of the fourth phase (from 394 to 453°C) was augmented significantly with WPU addition level increasing, which implied that the polyol content was increasing, and with the temperature ascending, the degradation of polyols intensified resulting in the growth of the maximum weight loss rate. What is more, this discovery was in line with the results published by Somani et al. [22]. Table 2 provides the maximum weight loss speeds and the characteristic temperatures. The characteristic temperatures of the first two phases were decreasing

with varying degrees, and the corresponding maximum weight loss rate decreased significantly. Moreover, in the third phase of SFAs with WPU modification, the characteristic temperature was growing dramatically, indicating the enhancement of polymers generated by the cross-linking reactions between the WPU and soy protein molecule. After cross-linking reactions, modified SFAs obtained better thermal stability than did pristine SFAs, and the degradation process was shifting to a higher-temperature area. This was verified by the decline in the maximum weight loss rates described above.

3.4. Analysis of Curing Kinetics. Through analyzing TG-DTG curves of the curing process of soy-based adhesives, it could be divided into 2 to 4 phases, assuming that these phases were in line with the first-order reaction process. Then, the curing kinetics equation under a constant heating rate calculated by the Coats-Redfern integral method was given by equation (2), and the adhesive conversion ratio was calculated by equation (1).

$$x = \frac{m_0 - m_t}{m_0 - m} \times 100\%, \quad (1)$$

$$\frac{dx}{dt} = A \exp\left(-\frac{E}{RT}\right)(1-x), \quad (2)$$

where x (%) is the adhesive conversion ratio, m_0 (mg) is the initial sample weight, m_t is the sample weight of the

TABLE 3: Parameters of reaction kinetics of different adhesive samples.

Samples	Temperature (°C)	Fitting equation	Activation energy (kJ·mol ⁻¹)	Preexponential factor (s·mol·l ⁻²)	Correlation coefficient
SFA	52~147	$y = -3391.9x - 5.6499$	46.98	1.61×10^4	0.9848
	147~387	$y = -5708x - 3.6775$	30.58	1.45×10^3	0.9311
SFA-WPU5	57~146	$y = -5708x - 3.6775$	82.98	2.15×10^6	0.9723
	146~257	$y = -1912.2x - 10.595$	88.09	4.23×10^6	0.9921
	257~357	$y = -4419.7x - 6.0021$	49.9	2.42×10^4	0.983
	357~417	$y = -514.82x - 12.459$	54.11	3.2×10^7	0.9866
SFA-WPU10	54~149	$y = -2187.1x - 9.4573$	78.63	1.21×10^6	0.9647
	149~267	$y = -2374.8x - 9.6585$	80.31	1.51×10^6	0.922
	267~347	$y = -4672.1x - 5.6689$	47.13	1.64×10^4	0.9919
	347~450	$y = -1676.3x - 10.658$	78.62	4.53×10^6	0.9743
SFA-WPU15	50~135	$y = -2059.4x - 9.7389$	80.97	1.65×10^6	0.9816
	135~242	$y = -2428.1x - 9.65$	80.23	1.5×10^6	0.9746
	242~380	$y = -5226.3x - 4.7039$	49.11	5.19×10^3	0.9911
	380~481	$y = -6029.2x - 3.9818$	89.11	2.13×10^3	0.991
SFA-WPU20	55~134	$y = -2417.5x - 8.7553$	72.8	5.55×10^5	0.9603
	134~253	$y = -2158.1x - 10.312$	85.74	1.7×10^6	0.961
	253~385	$y = -4989.7x - 5.2923$	44	1.05×10^4	0.9519
	385~488	$y = -5377.1x - 5.1457$	100.78	8.83×10^3	0.9723

corresponding curing time, m is the sample weight of termination temperature, E (J/mol) is the activation energy, A (s·mol/l²) is the preexponential factor; and T (K) is the temperature.

For a constant heating rate, assuming $H = dT/dt$, equation (3) can be calculated from the integral of equation (2).

$$\ln \left[\frac{-\ln(1-x)}{T^2} \right] = \ln \left[\frac{AR}{HE} \left(1 - \frac{2RT}{E} \right) \right] - \frac{E}{RT}. \quad (3)$$

As illustrated in equation (3), $\ln [AR/HE(1 - (2RT/E))]$ is almost constant. When the reaction order is 1, the graph plotted by $\ln [-\ln(1-x^2)/T^2]$ and $1/T$ is a straight line. Consequently, based on the slope and intercept of the straight line, the preexponential factor and the activation energy can be calculated.

Table 3 provides the curing kinetic parameters of soy-based adhesives obtained by linear regression according to the relationship diagram at different phases. It could be concluded from Table 3 that the kinetic parameters of this experiment had a high correlation coefficient, which illustrated that the first-order reaction kinetic model was feasible. In addition, compared with SFAs, with the rising addition level of WPU, the activation energy of the corresponding phases increased to varying degrees, and the activation energy of the third phase of SFAs modified with different addition levels of WPU was increased by 63%, 54%, 61%,

and 44%, respectively, corresponding to the second phase of pristine SFAs. It was revealed that the reactivity of SFAs with WPU modification was weakened and the reason of the growth of the characteristic temperature was confirmed. In addition, the curing temperatures of modified SFAs were higher than those of pristine SFAs.

4. Conclusions

The pristine SFAs during the hot curing process can be divided into two phases. The first phase was mainly the evaporation of small molecule and organic compounds (from 30 to 148°C), and the second phase was the decomposition of carbohydrates and protein (from 258 to 380°C). However, the curing process of SFAs with WPU modification was totally different from that of pristine SFAs which can be split into four phases. The first phase was from 30 to 138°C, which was mainly attributed to the evaporation of small molecule and organic compounds, and the cross-linking reaction between soy protein and WPU was taking place in this phase. The second phase, mainly from 186 to 220°C, was attributed to the evaporation and curing of a small molecule polymer of WPU. The third phase occurred at 286 to 342°C, which was mainly ascribed to the decomposition of polysaccharides, soy protein, and polymers formed between WPU and soy protein. And the fourth phase occurred at 394 to 453°C, which contributed to the decomposition of polyols of WPU. Due to the addition of WPU, the curing property of

SFAs had a significant difference. In addition, the kinetics calculation results demonstrated that the curing procedures were in accordance with the first-order reaction process. Moreover, the analysis by the curing process indicated that the addition of WPU improved the stability of SFAs that can make the activation energy at different phases improve to varying degrees.

Data Availability

The data used to support the findings of this study are available from the corresponding author upon request.

Conflicts of Interest

The authors declare that they have no competing interests.

Acknowledgments

This work is supported by the grant from Major Science and Technology Special Project in Hunan (2017NK1010) and Forestry Science and Technology Demonstration Project Funds of Central Finance (2016[XT] 006).

References

- [1] J. Sun, L. Li, H. Cheng, and W. Huang, "Preparation, characterization and properties of an organic siloxane modified cassava starch-based wood adhesive," *Journal of Adhesion*, vol. 94, no. 4, pp. 278–293, 2017.
- [2] Q. Xu, J. Wen, and Z. Wang, "Preparation and properties of cassava starch-based wood adhesives," *BioResources*, vol. 11, no. 3, pp. 6756–6767, 2016.
- [3] J. M. Raquez, M. Deléglise, M. F. Lacrampe, and P. Krawczak, "Thermosetting (bio)materials derived from renewable resources: a critical review," *Progress in Polymer Science*, vol. 35, no. 4, pp. 487–509, 2010.
- [4] J. Li, J. Luo, X. Li, Z. Yi, Q. Gao, and J. Li, "Soybean meal-based wood adhesive enhanced by ethylene glycol diglycidyl ether and diethylenetriamine," *Industrial Crops and Products*, vol. 74, pp. 613–618, 2015.
- [5] T. Wu and R. Farnood, "A preparation method of cellulose fiber networks reinforced by glutaraldehyde-treated chitosan," *Cellulose*, vol. 22, no. 3, pp. 1955–1961, 2015.
- [6] S. Damodaran and D. Zhu, "A formaldehyde-free water-resistant soy flour-based adhesive for plywood," *Journal of the American Oil Chemists' Society*, vol. 93, no. 9, pp. 1311–1318, 2016.
- [7] Y. Jang and K. Li, "An all-natural adhesive for bonding wood," *Journal of the American Oil Chemists' Society*, vol. 92, no. 3, pp. 431–438, 2015.
- [8] N. S. Hettiarachchy, U. Kalapathy, and D. J. Myers, "Alkali-modified soy protein with improved adhesive and hydrophobic properties," *Journal of the American Oil Chemists' Society*, vol. 72, no. 12, pp. 1461–1464, 1995.
- [9] H. N. Xu, Q. Y. Shen, X. K. Ouyang, and L. Y. Yang, "Wetting of soy protein adhesives modified by urea on wood surfaces," *European Journal of Wood and Wood Products*, vol. 70, no. 1–3, pp. 11–16, 2012.
- [10] Q. Lin, N. Chen, L. Bian, and M. Fan, "Development and mechanism characterization of high performance soy-based bio-adhesives," *International Journal of Adhesion and Adhesives*, vol. 34, no. 4, pp. 11–16, 2012.
- [11] K. Gu and K. Li, "Preparation and evaluation of particleboard with a soy flour-polyethylenimine-maleic anhydride adhesive," *Journal of the American Oil Chemists' Society*, vol. 88, no. 5, pp. 673–679, 2011.
- [12] C. Gui, G. Wang, D. Wu, J. Zhu, and X. Liu, "Synthesis of a bio-based polyamidoamine-epichlorohydrin resin and its application for soy-based adhesives," *International Journal of Adhesion and Adhesives*, vol. 44, no. 10, pp. 237–242, 2013.
- [13] G. Qi, N. Li, D. Wang, and X. S. Sun, "Physicochemical properties of soy protein adhesives modified by 2-octen-1-ylsuccinic anhydride," *Industrial Crops and Products*, vol. 46, pp. 165–172, 2013.
- [14] H. Liu, C. Li, and X. S. Sun, "Improved water resistance in undecylenic acid (UA)-modified soy protein isolate (SPI)-based adhesives," *Industrial Crops and Products*, vol. 74, pp. 577–584, 2015.
- [15] S. D. Desai, J. V. Patel, and V. K. Sinha, "Polyurethane adhesive system from biomaterial-based polyol for bonding wood," *International Journal of Adhesion and Adhesives*, vol. 23, no. 5, pp. 393–399, 2003.
- [16] H. Chen and N. Yan, "Application of western red cedar (*Thuja plicata*) tree bark as a functional filler in pMDI wood adhesives," *Industrial Crops and Products*, vol. 113, pp. 1–9, 2018.
- [17] Y. Wang, Y. Fan, L. Deng, Z. Li, and Z. Chen, "Properties of soy-based wood adhesives enhanced by waterborne polyurethane modification," *Journal of Biobased Materials and Bioenergy*, vol. 11, no. 4, pp. 330–335, 2017.
- [18] H. N. Cheng, C. Ford, M. K. Dowd, and Z. He, "Soy and cottonseed protein blends as wood adhesives," *Industrial Crops and Products*, vol. 85, pp. 324–330, 2016.
- [19] G. Qi and X. S. Sun, "Soy protein adhesive blends with synthetic latex on wood veneer," *Journal of the American Oil Chemists' Society*, vol. 88, no. 2, pp. 271–281, 2011.
- [20] Y. Wang, X. Mo, X. S. Sun, and D. Wang, "Soy protein adhesion enhanced by glutaraldehyde crosslink," *Journal of Applied Polymer Science*, vol. 104, no. 1, pp. 130–136, 2007.
- [21] C. Wayakron Phetphaisit, R. Bumee, J. Namahoot, J. Ruamcharoen, and P. Ruamcharoen, "Polyurethane polyester elastomer: innovative environmental friendly wood adhesive from modified PETs and hydroxyl liquid natural rubber polyols," *International Journal of Adhesion and Adhesives*, vol. 41, no. 1, pp. 127–131, 2013.
- [22] K. P. Somani, S. S. Kansara, N. K. Patel, and A. K. Rakshit, "Castor oil based polyurethane adhesives for wood-to-wood bonding," *International Journal of Adhesion and Adhesives*, vol. 23, no. 4, pp. 269–275, 2003.
- [23] M. Zhang, F. Song, X. L. Wang, and Y. Z. Wang, "Development of soy protein isolate/waterborne polyurethane blend films with improved properties," *Colloids and Surfaces B: Biointerfaces*, vol. 100, no. 100, pp. 16–21, 2012.
- [24] D. Ren and C. E. Frazier, "Structure–property behavior of moisture-cure polyurethane wood adhesives: influence of hard segment content," *International Journal of Adhesion and Adhesives*, vol. 45, no. 2, pp. 118–124, 2013.
- [25] C. Wang, Y. Wang, W. Liu et al., "Natural fibrous nanoclay reinforced soy polyol-based polyurethane," *Materials Letters*, vol. 78, no. 7, pp. 85–87, 2012.

- [26] C. Wang, L. Ding, Q. Wu et al., "Soy polyol-based polyurethane modified by raw and silylated palygorskite," *Industrial Crops and Products*, vol. 57, pp. 29–34, 2014.
- [27] D. Ren and C. E. Frazier, "Structure/durability relationships in polyurethane wood adhesives: neat films or wood/polyurethane composite specimens," *International Journal of Adhesion and Adhesives*, vol. 45, no. 9, pp. 77–83, 2013.

